Spike-based Neuromorphic Model for Sound Source Localization

Dehao Zhang[1,‡], **Shuai Wang**[1,‡], **Ammar Belatreche**[2], **Wenjie Wei**[1], **Yichen Xiao**[1], **Haorui Zheng**[3], **Zijian Zhou**[1], **Malu Zhang**[1,*], **Yang Yang**[1]
[1] University of Electronic Science and Technology of China
2 Northumbria University
3 Peking University
{zhangdh,wangshuai718}@std.uestc.edu.cn, maluzhang@uestc.edu.cn

Abstract

Biological systems possess remarkable sound source localization (SSL) capabilities that are critical for survival in complex environments. This ability arises from the collaboration between the auditory periphery, which encodes sound as precisely timed spikes, and the auditory cortex, which performs spike-based computations. Inspired by these biological mechanisms, we propose a novel neuromorphic SSL framework that integrates spike-based neural encoding and computation. The framework employs Resonate-and-Fire (RF) neurons with a phase-locking coding (RF-PLC) method to achieve energy-efficient audio processing. The RF-PLC method leverages the resonance properties of RF neurons to efficiently convert audio signals to time-frequency representation and encode interaural time difference (ITD) cues into discriminative spike patterns. In addition, biological adaptations like frequency band selectivity and short-term memory effectively filter out many environmental noises, enhancing SSL capabilities in real-world settings. Inspired by these adaptations, we propose a spike-driven multi-auditory attention (MAA) module that significantly improves both the accuracy and robustness of the proposed SSL framework. Extensive experimentation demonstrates that our SSL framework achieves state-of-the-art accuracy in SSL tasks. Furthermore, it shows exceptional noise robustness and maintains high accuracy even at very low signal-to-noise ratios. By mimicking biological hearing, this neuromorphic approach contributes to the development of high-performance and explainable artificial intelligence systems capable of superior performance in real-world environments.

1 Introduction

Sound source localization (SSL) [11, 43] is a critical skill for mammals that enables them to identify and locate external auditory stimuli. This skill plays a vital role in survival behaviors like prey detection and predator evasion. Over decades of scientific exploration [39, 48], SSL has evolved from a purely biological concept to a sophisticated technology with a wide range of applications across various fields [10, 39]. Today, SSL methods are finding increasing use in areas like security monitoring [12], robotic navigation [37], and autonomous driving [13, 36].

Early SSL approaches rely on hand-crafted analysis of speech signals from multiple receivers. While offering a basic ability to localize sound sources, these methods suffer from limitations in accuracy and robustness. The emergence of Deep Neural Networks (DNNs) and their success in various domains lead researchers to explore their application in SSL tasks, achieving significant performance improvements [64, 67]. However, DNN-based approaches face two key challenges. Firstly, DNNs

[*‡] Equal contribution, * Corresponding author

38th Conference on Neural Information Processing Systems (NeurIPS 2024).

achieving high SSL accuracy often require substantial computational resources, leading to increased energy consumption. Secondly, DNNs struggle to learn the intricate relationships between localization behaviors and noisy environmental constraints. These limitations hinder the development of portable, edge-based SSL models [16] for real-world environments.

Recently, Spiking Neural Networks (SNNs) [14, 20, 34], inspired by brain neural architectures, have gained significant attention for their energy-efficient simulation of neural systems. Spiking neurons [33] simulate the information transmission mechanism of biological neurons, computing only upon the arrival of input spikes and remaining silent otherwise [53]. Such an event-driven mechanism results in sparser information transmission [60, 61], hence reducing computational costs [6, 69]. Therefore, the SNN-based SSL models enable a more energy-efficient emulation of biological SSL processes. Pan et al. [40] propose a SNN-based SSL model that achieves localization in real audio signals. Chen et al.[7] improve the model's performance through a hybrid encoding method, achieving competitive results with less energy consumption. Although these examples achieve edge-friendly SSL ability, limitations still exist in neural encoding efficiency and robustness under noisy conditions.

In terms of neural encoding, most methods still rely on Fourier Transform (FT) [27, 55] to encode ITD [11] present in the received audio signals into spike trains for processing by back-end SSL model. However, FT operations involve many multiply-accumulate (MAC) computations and require significant computational resources [58] which hinders our goal of developing energy-efficient SSL models. In terms of robustness, the superior localization ability in biology not only relies on ITD cues but also on various auditory mechanisms [22, 54], such as frequency preferences, short-term memory, etc. Frequency preference significantly mitigates the impact of complex environments on localization accuracy [31, 62], and auditory short-term memory effectively filters out irrelevant noise [49, 50], focusing on important auditory signals. However, most SNN-based solutions [3, 32] primarily focus on ITD cues, with little attention to multiple auditory mechanisms. Therefore, investigating more energy-efficient and robust SNN-based SSL models remains a pressing challenge to address.

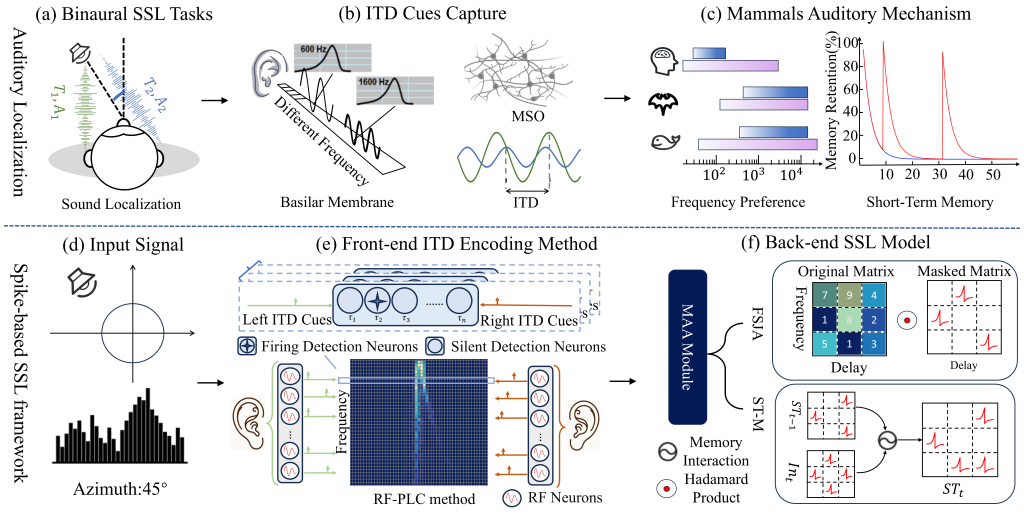

Figure 1: A spike-based SSL framework inspired by biological auditory localization. (a) Schematic of binaural SSL tasks. (d) Simulation of the SSL tasks. The upper section illustrates two key processes involved in mammalian localization: (b) the Basilar Membrane and Medial Superior Olive (MSO) collaborate to capture ITD cues; (c) multiple auditory attention mechanisms further process these ITD cues for precise localization. The lower section presents our spike-based SSL framework, comprising two main components: (e) a front-end ITD encoding method employing RF and detection neurons; (f) A back-end SSL model utilizing multi-auditory attention.

In this paper, we propose a novel SNN-based SSL framework, which primarily comprises an ITD encoding front-end method and a biomimetic localization back-end model. As illustrated in Fig.1, we introduce a phase-locking coding (RF-PLC) method using Resonate-and-Fire (RF) neurons [8, 38] and detection neurons [40]. It simulates the frequency band decomposition function of the basilar membrane and captures ITD cues, respectively. Furthermore, we introduce a novel back-end SSL model based on multi-auditory attention (MAA) that integrates frequency preferences and short-term

memory characteristics. This approach significantly improves both the accuracy and robustness of localization. Extensive experiment on the HRTF [57], Single Words [30], and SLoClas [42] datasets demonstrates that our SNN-based model achieves state-of-the-art performance. Moreover, evaluation in noisy environments reveals the model's enhanced adaptability to real-world conditions. The work introduces the following key contributions:

- **Spike-based ITD encoding**: The RF-PLC method leverages the resonance properties of RF neurons to perform energy-efficient auditory time-frequency transformations, avoiding the high resource costs of FT operations. Additionally, it utilizes a phase-locking loop and ITD detection neurons to encode auditory ITD cues into spike patterns directly, ensuring the fully spike-driven nature of the entire SSL framework.
- **Biologically inspired attention**: The MAA module incorporates knowledge of biological auditory frequency preferences and short-term memory characteristics. Frequency preferences effectively mask the ITD information of irrelevant frequency bands and spatial regions, while short-term memory focuses on the interaction of information across adjacent time steps. This combination enhances the robustness of the SNN model in noisy environments.
- **State-of-the-art performance with reduced complexity**: By integrating these methods, we present a SNN-based SSL framework that achieves state-of-the-art performance while reducing energy consumption to existing works. Additionally, extensive experimentation demonstrates that our system exhibits superior robustness in noisy environments.

2 Related Work

2.1 ITD Cues for SSL Tasks

To develop biologically inspired models for SSL tasks, researchers have drawn upon the auditory localization mechanisms observed in mammals [23, 25]. The cues of ITD are recognized as critical for these models [29, 44, 46, 47]. ITD refers to the temporal disparity in sound arrival between the ears. Specifically, when a sound source is closer to the listener's right side, audio reaches the right ear sooner than the left. The Jeffress model [3] and BiSoLaNN [56] encode ITD cues into spike trains and corroborate their biological credibility through experiments on barn owls [5]. But these approaches primarily focus on the localization of pure tones, which significantly differs from the time-varying audio signal in daily life. Substantially, some researchers [7, 40] have utilized complex FT operations to obtain the phase information of audio signals. However, FT operations require substantial computational resources and pose significant challenges when implementing systems on edge devices with limited computational capabilities. Therefore, the exploration of low-power ITD encoding methods become a pressing direction to pursue.

2.2 Biological Adaptation in Auditory System

In the field of auditory science, frequency preference and short-term memory characteristics are essential for understanding auditory processing. Numerous studies [21, 52, 63] have demonstrated that biological auditory systems exhibit heightened sensitivity to specific frequency ranges, such as 20-20 000 Hz in humans, with other species like bats and blue whales adapted to different ranges. Further research [51] has revealed tonotopic maps and variations in frequency tuning across regions, underscoring the importance of frequency selectivity in hearing. Electrophysiological experiments [31] confirmed that inner hair cells on the basilar membrane of the cochlea exhibit significant differences in response to various frequency bands.

These studies underscore the irreplaceable role of frequency band preference in auditory decision-making. Additionally, compared to visual short-term memory, auditory short-term memory [2, 28] has a shorter retention span. Nonetheless, it is essential for real-time integration and coherent environmental perception. Simultaneously, some researchers [50] propose that neurofeedback training targeting auditory short-term memory can significantly enhance selective attention to auditory signals in noisy environments. Moreover, Zhong et al. [70] suggested that auditory short-term memory can highlight sound source characteristics under reverberant conditions, reducing interference from other sources. However, current SSL methods mainly focus on ITD cues, neglecting these well-established biological mechanisms. Therefore, the effective integration of diverse auditory attention mechanisms within SSL tasks to enhance robustness remains a significant ongoing challenge.

3 Method

In this section, we introduce our spike-based SSL framework, which includes a front-end ITD encoding method and a back-end localization model. For the front-end ITD encoding, we propose the energy-efficient RF-PLC method, which uses RF neurons to capture ITD cues and detection neurons to convert these encoded cues into spike patterns. For the back-end localization model, we take inspiration from biological adaptation and propose the MAA mechanism to enhance the model's localization performance and robustness.

3.1 RF Phase-locking Coding: A Direct Font-end ITD Encoding Method

Due to the physical separation of the ears, sound waves arrive at each ear with slightly different timing. It leads to differences in the initial phase information between the two audio channels. Pan et al. [40] propose a Multi-Tones Phase Coding (MTPC) method that utilizes this information to exploit ITD cues. However, this approach relies on computationally expensive FT operations and introduces an additional phase transformation step during processing. To overcome these limitations, we propose the RF-PLC method, leveraging RF neurons' resonance filtering and periodic decay properties. This approach effectively eliminates the need for energy-intensive FT and phase transformation processes. Subsequently, a set of detection neurons with varying delays is employed to efficiently encode the ITD cues from different microphones into spike patterns.

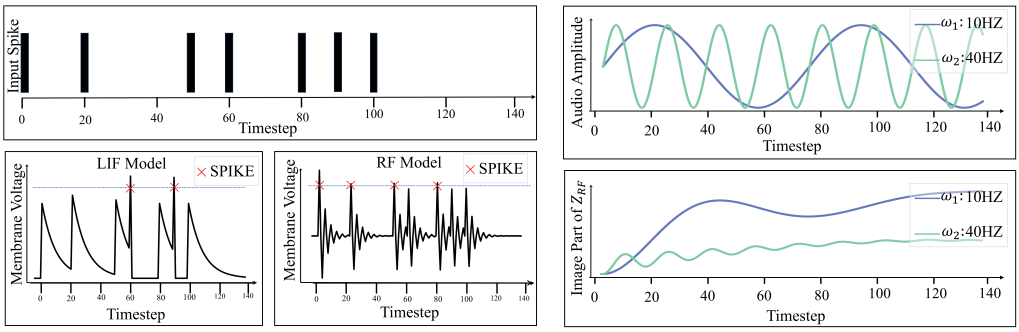

(a) (b)

Figure 2: Properties of spiking neuron models. (a) Responses of the LIF and RF neurons to an identical input spike train. We can observe distinct patterns in both membrane voltage accumulation and spiking behavior between the two neuron models. (b) The frequency-selective properties of RF neurons. RF neurons with a resonant frequency of 10 Hz ($\omega = 10$) have a significantly stronger response at 10 Hz compared to the response at 40 Hz.

The first step of our model processes the raw audio to capture ITD cues. We segment the audio into y_l based on the smallest durations by the human ear. These segments are then encoded by specialized RF neurons [38] tuned to different frequency bands. The dynamics of these RF neurons can be described as follows:

$$\mathcal{Z}_{\text{RF}}[t] = \lambda e^{\mathrm{i}\omega\Delta t}\mathcal{Z}_{\text{RF}}[t-1] + I[t], \tag{1}$$

where ω represents the resonant frequency of the neuron, indicating the number of radians it progresses per second. λ serves as the dampening factor, which causes the oscillation to decay exponentially. Δt represents the sampling rate, which is set to 1. $I[t]$ denotes the audio input. $\mathcal{Z}_{\text{RF}}[t]$ can be reformulated as $x + \mathrm{i}y \in \mathbb{C}$. A detailed process can be found in Appendix. A. The real component x of $\mathcal{Z}_{\text{RF}}$ reflects the current-like behavior of the neuron, capturing the dynamics of voltage-gated and synaptic currents. The imaginary component y of $\mathcal{Z}_{\text{RF}}[t]$ serves as a voltage-like variable.

Based on Eq. 1, we depict the spiking behavior of the RF neuron in Fig. 2(a) and summarize its characteristics in two aspects. Firstly, the complex form of the RF neuron's dynamics enables it to capture the phase information in a specific frequency band ω, termed resonance filtering. Secondly, the dampening factor λ allows it to exhibit periodic decay characteristics when there is no input.

By leveraging RF neurons' resonance filtering and periodic decay properties, we encode input signals into ITD cues efficiently and effectively. To better describe the RF-PLC process, we decompose the

dynamics of the RF neurons into two stages: a silent stage and a spike stage. The silent stage is utilized to decompose audio information into distinct frequency components and store this data in the state of the RF. The spike stage then oscillates phase information, effectively converting it into ITD cues through phase-locking mechanisms. These stages can be described as follows:

$$\mathcal{Z}_{\mathrm{RF}}[t] = \begin{cases} e^{\mathrm{i}\omega\Delta t}\mathcal{Z}_{\mathrm{RF}}[t-1] + I[t], & \text{Silent Stage,} \\ \lambda e^{\mathrm{i}\omega\Delta t}\mathcal{Z}_{\mathrm{RF}}[t-1], & \text{Spike Stage.} \end{cases} \tag{2}$$

In the silent stage, RF neurons with distinct ω values selectively respond to specific resonant frequencies. As illustrated in Fig.2(b), when the frequency ω_1 of the audio input $I[t]$ closely matches the RF neuron's resonant frequency ω, a significant increase in its membrane potential occurs. Conversely, misalignment between these frequencies leads to a slower accumulation of membrane potential. This characteristic offers an energy-efficient alternative to the computationally expensive FT operations. The result of the silent stage can be interpreted as analogous to the initial phase information of each pure sinusoidal component within the audio signal.

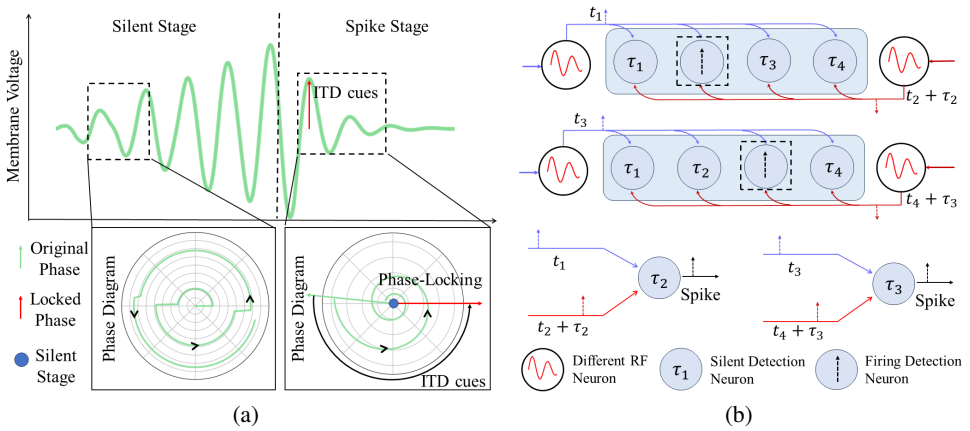

Figure 3: The proposed the RF-PLC method. (a) ITD cues capture: during the silent stage, RF neurons replace FT by responding to input signals. In the spike stage, the RF neurons' first oscillatory peak time is encoded as their spike firing time through a phase-locking loop. (b) The coincidence detection network: detection neurons directly encode ITD cues by analyzing the spike timings of multiple RF neurons from two receivers and generating spikes after a specific time delay.

In the spike stage, we introduce a PLC method that ensures the RF neuron fires a spike only at a specific phase. Specifically, the spike firing time t_{lock} is defined as the special state when the real part of the RF neuron state reaches zero and the imaginary part reaches its maximum ($\mathcal{Z}_{\mathrm{RF}}[t_{\mathrm{lock}}] = 0 + \mathrm{i}y_{\max}$). This precise spike timing can be directly utilized as an ITD cue, with details validated in Appendix B. Notably, the periodic decay characteristic of RF neurons guarantees that only one spike is generated using our PLC method, ensuring the efficiency of ITD encoding.

As illustrated in Fig. 3(a), we provide a schematic representation for obtaining ITD cues from input audio. During the silent stage, RF neurons receive audio signals and convert them into phase information of pure tones at different frequencies. During the spike stage, the PLC method leverages this phase information to determine whether the RF neuron fires a spike. The precise spike timing of the RF neuron serves as the ITD cue. Compared to traditional FT-based methods that rely on multiple network layers, our RF-PLC significantly reduces computational costs and offers a more biologically plausible representation of ITD cues.

The final step of the RF-PLC method involves detection neurons that convert spike times (also, ITD cues) into spike patterns. As illustrated in Fig. 3(b), a series of detection neurons are used in each band, with each neuron tuned to a specific delay preference (from τ_1 to τ_n). These detection neurons then encode the overall ITD cues for the audio signal. Interestingly, similar symmetrical detection structures have been observed in mammalian auditory pathways [15], which support the biological plausibility of our approach.

3.2 MAA: Multi-auditory Attention Mechanism for Back-end SNN-based SSL Model

After encoding audio signals into spike patterns, we construct a back-end SNN-based model to process this encoded information for SSL tasks. The SNN-based SSL model is built based on the Leaky Integrate-and-Fire (LIF) neuron due to its computation efficiency. The LIF model receives the resultant current and accumulates membrane potential which is used to compare with the threshold to determine whether to generate the spike. Its dynamic can be described as follows:

$$U[t+1] = H[t] + X[t+1], \tag{3}$$

$$S[t+1] = \Theta(U[t+1] - V_{th}), \tag{4}$$

$$H[t+1] = V_{reset}S[t+1] + \tau U[t+1](1 - S[t+1]). \tag{5}$$

At each time step $t+1$, the spatial input current $X[t+1]$ is obtained through convolution and linear layers. This current integrates with the previous temporal input $H[t]$ to update the membrane potential $U[t+1]$. The Heaviside step function $\Theta(\cdot)$ determines whether the binary spike $S[t+1]$ is generated by comparing the membrane voltage with the threshold V_{th}.

If there is spike emission, $H[t]$ is reset to the resting potential V_{reset}; otherwise, $U[t+1]$ decays with a time constant τ and directly feeds into $H[t+1]$. We denote the LIF spiking neuron layer as $\mathcal{SN}(\cdot)$, which takes $X[t+1]$ as input and produces the spike tensor $S[t+1]$ as output. Existing back-end SNN-based SSL models only rely on simple convolutional and fully connected layers for localization, without considering biological adaptation mechanisms such as frequency band selectivity and short-term memory. This leaves substantial room for improvement in localization performance. Therefore, we draw on these biological mechanisms to propose the computationally efficient MAA.

In the field of SNNs, there have been some studies on attention mechanisms [19, 65, 71]. However, these methods almost rely heavily on squeeze-and-excitation operations, which introduce additional MAC operations. Therefore, we propose a novel spike-driven MAA mechanism that comprises a frequency-spatial joint attention module and a short-term memory structure. The former enhances networks' focus on critical ITD cues within key frequency bands. The latter strengthens the model's memory for wise decisions across timeframes. Notably, our MAA module is tailored for SSL tasks and achieves the best trade-off between performance and efficiency.

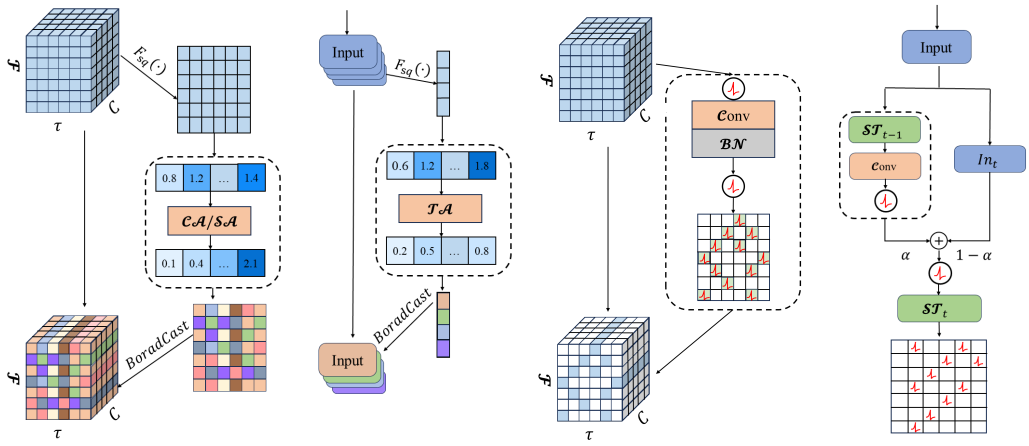

(a) Spatial Attention in SNNs (b) Time Attention (c) FSJA module (ours) (d) ST-M (ours)

Figure 4: Comparing MAA with spiking attention methods. (a) In SNNs, CA/SA[66] uses MAC-based broadcasting operations. (b) TA [65] efficiently focuses on temporal sequences but struggles with streaming data. (c) FSJA adopts a binary attention map as an alternative to MAC-based broadcasting, enhancing computational sparsity and masking noise (white blocks). (d) ST-M incorporates ITD cues within a streaming context, significantly reducing the model's computational resource.

3.2.1 Frequency-Spatial Joint Attention

To enhance adaptive learning and selection of preferred frequency in our SNN-based SSL model, we propose a spike-driven FSJA module. For each time step, the output of the RF-PLC method is

defined as $X[t] \in \mathbb{R}^{C \times \mathcal{F} \times \mathcal{S}}$, where $\mathcal{F}$ and $\mathcal{S}$ respectively represent the number of RF and detection neurons, and C denotes the microphone array. The FSJA module can be expressed as follows:

$$\mathcal{Z} = \mathcal{SN}(\frac{1}{\mathcal{F} \times \mathcal{S}} \sum_{i=1}^{\mathcal{F}} \sum_{j=1}^{\mathcal{S}} X_{i,j}[t]), \text{Att}_{FS}(\mathcal{Z}) = \mathcal{SN}(\text{ConvBN}(\mathcal{Z})), \text{FSJA} = \text{Att}_{FS}(\mathcal{Z}) \cdot X[t], \quad (6)$$

where ConvBN is convolution operations with a 3×3 kernel and batch normalization. The matrix $\mathcal{Z}$ is defined as the average of $X[t]$ across the $\mathcal{F}$ dimension and $\mathcal{S}$ dimension and the spike results after passing through the LIF neuron. Due to the attention map of FSJA module is in binary spike form, it effectively concentrates on spike information at specific frequency and spatial dimensions.

To further demonstrate the difference between our FSJA module and previous SNN-based attention methods across frequency and spatial dimensions, we show the difference between them. As shown in Fig. 4(a), the existing SNN-based attention module relies on full-precision values. Although the broadcast operation is a spike-driven computational paradigm, it introduces additional MAC operations for the next layer. As shown in Fig. 4(c), it effectively avoids MAC-based broadcasting operations which substantially improves energy efficiency. Additionally, our method effectively masks the ITD information of irrelevant frequency bands and spatial regions, substantially boosting the SSL model's robustness in noisy environments.

3.2.2 Short-term Memory Structure

The auditory short-term memory characteristic enables sustained perception of SSL processing, yet few studies have focused on this aspect. Although the membrane potential accumulation of spiking neurons partially reflects this mechanism, its simplified mathematical expression is insufficient for describing short-term memory adequately. Therefore, we develop an innovative ST-M structure that emphasizes the interaction of information across adjacent time steps to enhance the neuronal memory capacity. The structure can be represented as:

$$\begin{aligned} In[t] &= \mathcal{SN}(\text{ConvBN}(X[t])), \\ \mathcal{ST}[t] &= \mathcal{SN}(\alpha \, \text{ConvBN}(\mathcal{ST}[t-1]) + (1-\alpha) \, In[t]), \end{aligned} \quad (7)$$

where $In[t]$ represents the preliminary feature extraction of the input $X[t]$, and $\mathcal{ST}[t]$ denotes the enhanced memory unit, with α serving as the hyperparameter that balances adjacent time steps. Our ST-M architecture is asynchronous, processing information frame-by-frame rather than employing time-dimension attention, thereby significantly reducing the computational resources required by the network and facilitating the direct processing of streaming audio information. Additionally, by balancing the memory residual at time $t-1$ with the input information at time t, our approach facilitates memory interaction between adjacent time steps. This processing paradigm that relies on input from adjacent time steps pays more attention to short-term memory, thereby granting our model improved localization robustness in dynamic environments.

To avoid the MAC operations present in $\alpha \, \text{ConvBN}(\mathcal{ST}[t-1])$, we integrate α into the firing threshold of $\mathcal{SN}$, which can be expressed by the following formula:

$$\mathcal{ST}[t] = \mathcal{SN}'\left(\text{ConvBN}(\mathcal{ST}[t-1]) + \frac{1-\alpha}{\alpha} In[t]\right). \quad (8)$$

Here, $\mathcal{SN}'$ denotes a layer of spiking neurons with a threshold of V_{th}/α. Due to $\mathcal{ST}[t]$ and $X[t]$ being binary spikes and ConvBN can be fused during inference, Eq. 8 contains no MAC operations which ensure low power consumption in inference. Compared with attention in the temporal dimension, the ST-M structure demonstrates asynchronous inference and low-power computational characteristics. As shown in Fig. 4(b) and Fig. 4(d), TA methods require the processing of all temporal information and rely on full-precision attention representation, whereas our ST-M structure utilizes only the spike information from adjacent time steps and features spike-driven computation. This ensures the model can perform inference in a low-power manner.

Combining the FSJA and ST-M modules, we propose a spike-driven MAA mechanism, with its insertion location detailed in the Appendix. D. The proposed MAA mechanism leverages the FSJA module to effectively filter noise, and the ST-M module to strengthen the model's memory for wise decisions across timeframes. As a result, our biologically inspired MAA significantly improves the localization accuracy and robustness of our SNN-based back-end network model.

4 Experiments

In this section, we evaluate our proposed spike-based SSL framework performance on three datasets: the HRTF [57], Single Words [30], and SLoClas dataset [42]. Moreover, we examine its energy efficiency and robustness through extensive ablation studies and noise addition experiments on the SLoClas dataset.

4.1 Comparison with SOTA Models

The HRTF dataset and Single Word are examined utilizing 2-channel audio at a singular frequency, with a minimum angular resolution of 10°. In contrast, the SLoClas dataset comprises 4-channel audio in real-world scenarios, with a higher resolution of 5°. Consequently, the SLoClas dataset presents a higher level of challenge and more closely resembles real-world scenarios. We report in detail the Mean Absolute Error (MAE) and the classification accuracy (Acc.) [7], defined as shows:

$$\begin{aligned} \mathrm{MAE}(^\circ) &= \frac{1}{N}\sum_{i=1}^{N}|\hat{\theta}_i - \theta|, \\ \mathrm{Acc.}(\%) &= \frac{1}{N}\sum_{i=1}^{N}(|\hat{\theta}_i - \theta| < \eta), \end{aligned} \tag{9}$$

where $\hat{\theta}_i$ represents the estimated azimuth angle, and θ_i denotes the ground truth azimuth angle of the sample i. MAE quantifies the deviation between predicted and true angles, where a lower value means superior performance. Moreover, Acc quantifies the similarity between predicted angles and actual output angles. The η is set differently across datasets to align with their specific characteristics: For the HRTF and Single Word datasets, η is set at 5°, while for the SLoClas dataset, it is set to 2.5°. In this manner, η is rounded to the nearest increment corresponding to the minimum localization resolution when calculating classification accuracy.

Table 1: Comparison of sound source localization systems.

Dataset	Methods	Type	Param (M)	T	DoA	
					MAE(°)	Acc(%)
HRTF	LSO [57]	SNN	-	-	-	74.56%
	MNTB [57]	SNN	-	-	-	97.38%
	Our works	SNN	1.64M	4	-	99.84%
Single Word	MSO/LSO [30]	SNN	-	-	-	96.30%
	Our works	SNN	1.64M	4	-	99.63%
SLoClas	GCC-PHAT [41]	ANN	4.17M	-	4.39°	86.94%
	SELDnet [1]	ANN	1.68M	-	1.78°	88.24%
	EINV2 [4]	ANN	1.63M	-	0.98°	94.64%
	SRP-DNN [64]	ANN	1.64M	-	0.96°	94.12%
	FN-SSL [59]	ANN	1.68M	-	0.63°	95.40%
	MTPC-CSNN [40]	SNN	1.61M	4	1.23°	93.95%
	MTPC-CSNN [40]	SNN	1.61M	8	1.02°	94.72%
	MTPC-RSNN [40]	SNN	1.67M	51	1.48°	94.30%
	Hybrid Coding [7]	SNN	1.61M	4.37	0.60°	95.61%
	Our works	SNN	1.64M	**4**	**0.33**° $\pm$ 0.02°	**96.40%** $\pm$0.3%

As shown in Table 1, our model achieves SOTA accuracy among similarly sized models but also significantly reduces MAE metrics. Specifically, our model achieves an accuracy of 99.84% and 99.63% on the HRTF datasets and Single Words, respectively. Additionally, on the challenging SLoClas dataset, our model achieves a MAE of 0.33° and an accuracy of approximately 96.4%, while the number of the model parameter is only 1.64M. It represents a nearly 50% improvement in the MAE metric compared to the current SOTA performance of SNN-based models. The localization precision of our model is also competitive compared to other recently introduced ANN models.

4.2 Ablation Study

To assess the efficiency of the proposed RF-PLC method and MAA module, we conduct a series of ablation studies. Specifically, we compare our ITD extraction approach in the RF-PLC method with the established FT-based method used in previous work [40]. As depicted in Fig.5(a), our method achieves an accuracy nearly identical to that of the conventional approaches, with an error rate of only 1%. Furthermore, prior research has demonstrated that RF neurons exhibit significantly lower energy consumption compared to FT operations, particularly when implemented on neuromorphic hardware [17, 18, 45]. These findings validate the effectiveness of our RF-PLC method in achieving a highly efficient and accurate ITD encoding scheme.

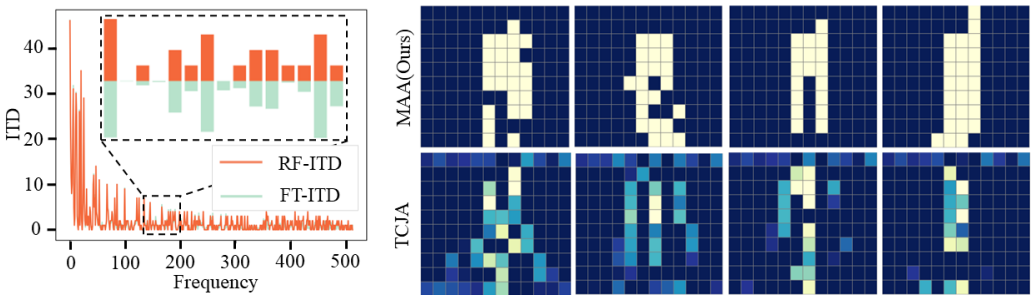

(a) (b)

Figure 5: (a) RF-PLF achieves results similar to FT-ITD, highlighting the benefit of avoiding FT operations in ITD encoding. (b) Attention mechanism. MAA's binary attention map effectively filters noise and avoids energy-intensive MAC-based broadcasting compared to other spiking attention.

The effectiveness of the MAA module is demonstrated in the model's localization performance. As shown in Table. 2, both the FSJA module and ST-M structure components individually enhance the performance of the back-end SSL model, and their combination yields even superior results. In addition, compared to attention mechanisms such as TA and TCJA, our attention method employs a fully spike-driven computational paradigm. This characteristic allows our MAA method to maintain an energy consumption of 9.58uJ, representing an increase of 8.49% compared to the work[40]. Moreover, Fig.5(b) illustrates the binary nature of the MAA attention map. This design effectively avoids the energy-intensive broadcasting operations typically associated with MAC units. Details on the energy consumption calculations are provided in Appendix. D and Appendix. E. This capability substantially improves the model's robustness, which is discussed in the following section.

Table 2: Ablation study

Methods	Spike-Driven	Param (M)	Power (uJ)	DoA	
				MAE (°)	Acc (%)
Baseline [40]	✓	1.61M	8.83	1.23°	93.95%
TA [66]	✗	1.62M	15.37	0.65°±0.05°	93.37% ±1.2%
TCJA [71]	✗	1.68M	15.34	0.47°±0.03°	93.45% ±1.0%
ST-M	✓	1.62M	8.99	0.45°±0.03°	95.67% ±0.5%
FSJA	✓	1.63M	9.42	0.49°±0.02°	95.95% ±0.6%
MAA	✓	1.64M	9.58	**0.33**°±0.02°	**96.40%**±0.3%

4.3 Robustness Experiments

To assess the robustness of our proposed spike-based SSL framework, we evaluate the distribution of MAE under varying signal-to-noise ratio (SNR) conditions. It is a metric used to measure the level of noise present in the input signal. It can be defined as follows:

$$\text{SNR (dB)} = 10 \cdot \log_{10} \left(\frac{P_{\text{signal}}}{P_{\text{noise}}} \right), \tag{10}$$

where P_{signal} represents the power of the signal and P_{noise} denotes the power of the noise. A lower SNR indicates a higher proportion of noise. Specifically, we incorporate noise from the NOISEX-92 database into audio recordings from different microphone channels. Detailed information about the noise addition process and the experimental setup is described in the Appendix.C.

As shown in Fig.6(a), we visualize the encoding results of the RF-PLC method under various SNR conditions to better understand the input form of our back-end model. In addition, we also present the distribution of recognition over 360°. As shown in Fig.6(b) and Fig.6(c), the MTPC method is more likely to predict certain angles, especially in terms of information in the noise direction; however, our method is not significantly affected by noise information. It indicates that our model exhibits higher stability. As SNR increases, our method demonstrates higher recognition accuracy. This indicates that our model effectively suppresses noise in specific frequency bands, thereby preventing significant variations in recognition results due to increased noise. The results provide strong evidence of the model's superior generalization and robustness when applied to complex real-world scenarios.

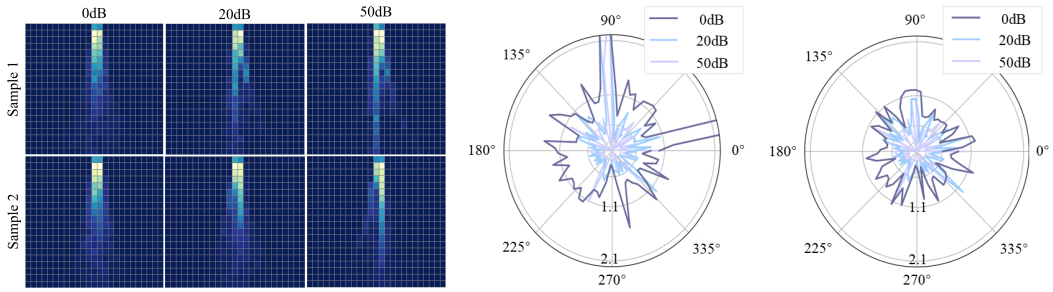

(a) (b) (c)

Figure 6: Performance under varying SNR levels. (a) Impact of SNR on ITD Encoding: at 0 dB, it is challenging to intuitively discern the direction of the sound source from the encoding results. (b) and (c) Different distribution of MAE over 360° in MTPC [40] and our model. Our model achieves enhanced noise resistance and improved localization stability.

5 Conclusion

Inspired by the efficiency of biological auditory systems, this work proposes a novel spike-based SSL framework. The core components are the RF-PLC method and the MAA module. The RF-PLC method leverages the resonance properties of RF neurons to bypass computationally expensive FT operations. It utilizes a phase-locking loop and ITD detection neurons to efficiently encode ITD cues from the audio signal into spike trains. Furthermore, the study incorporates insights from auditory biology, including frequency preferences and short-term memory characteristics. By designing a fully spike-driven MAA module, our SNN-based SSL model effectively filters irrelevant environmental noise in the frequency domain while temporally focusing on specific auditory content. This approach achieves superior performance, robustness, and interpretability, significantly advancing the field of neuromorphic SSL research. It establishes a new benchmark for the development of SSL techniques. Future work will investigate the deployment of this model on neuromorphic hardware platforms.

6 Acknowledgments

This work was supported in part by the National Natural Science Foundation of China under grant U20B2063, 62220106008, and 62106038, the Sichuan Science and Technology Program under Grant 2024NSFTD0034 and 2023YFG0259.

References

[1] Sharath Adavanne, Archontis Politis, Joonas Nikunen, and Tuomas Virtanen. Sound event localization and detection of overlapping sources using convolutional recurrent neural networks. *IEEE Journal of Selected Topics in Signal Processing*, 13(1):34–48, 2018.

[2] Amogh Agrawal, Aayush Ankit, and Kaushik Roy. Spare: Spiking neural network acceleration using rom-embedded rams as in-memory-computation primitives. *IEEE Transactions on Computers*, 68(8):1190–1200, 2019.

[3] Go Ashida and Catherine E Carr. Sound localization: Jeffress and beyond. *Current opinion in neurobiology*, 21(5):745–751, 2011.

[4] Yin Cao, Turab Iqbal, Qiuqiang Kong, Fengyan An, Wenwu Wang, and Mark D Plumbley. An improved event-independent network for polyphonic sound event localization and detection. In *ICASSP 2021-2021 IEEE International Conference on Acoustics, Speech and Signal Processing (ICASSP)*, pages 885–889. IEEE, 2021.

[5] Catherine E Carr and Masakazu Konishi. Axonal delay lines for time measurement in the owl's brainstem. *Proceedings of the National Academy of Sciences*, 85(21):8311–8315, 1988.

[6] Stefano Caviglia, Maurizio Valle, and Chiara Bartolozzi. Asynchronous, event-driven readout of posfet devices for tactile sensing. In *2014 IEEE International Symposium on Circuits and Systems (ISCAS)*, pages 2648–2651. IEEE, 2014. doi: 10.1109/iscas.2014.6865717 .

[7] Xinyi Chen, Qu Yang, Jibin Wu, Haizhou Li, and Kay Chen Tan. A hybrid neural coding approach for pattern recognition with spiking neural networks. *IEEE Transactions on Pattern Analysis & Machine Intelligence*, 46(05):3064–3078, 2024.

[8] Yi Chen, Hong Qu, Malu Zhang, and Yuchen Wang. Deep spiking neural network with neural oscillation and spike-phase information. In *Proceedings of the AAAI Conference on Artificial Intelligence*, volume 35, pages 7073–7080, 2021.

[9] James J Chrobak and Gyorgy Buzsáki. High-frequency oscillations in the output networks of the hippocampal–entorhinal axis of the freely behaving rat. *Journal of neuroscience*, 16(9):3056–3066, 1996.

[10] Maximo Cobos, Fabio Antonacci, Anastasios Alexandridis, Athanasios Mouchtaris, Bowon Lee, et al. A survey of sound source localization methods in wireless acoustic sensor networks. *Wireless Communications and Mobile Computing*, 2017, 2017.

[11] Dhwani Desai and Ninad Mehendale. A review on sound source localization systems. *Archives of Computational Methods in Engineering*, 29(7):4631–4642, 2022.

[12] Ha Manh Do, Karla Conn Welch, and Weihua Sheng. Soham: A sound-based human activity monitoring framework for home service robots. *IEEE Transactions on Automation Science and Engineering*, 19(3):2369–2383, 2021.

[13] Chuang Gan, Yiwei Zhang, Jiajun Wu, Boqing Gong, and Joshua B Tenenbaum. Look, listen, and act: Towards audio-visual embodied navigation. In *2020 IEEE International Conference on Robotics and Automation (ICRA)*, pages 9701–9707. IEEE, 2020.

[14] Wulfram Gerstner and Werner M Kistler. *Spiking neuron models: Single neurons, populations, plasticity*. Cambridge university press, 2002.

[15] Benedikt Grothe, Michael Pecka, and David McAlpine. Mechanisms of sound localization in mammals. *Physiological reviews*, 90(3):983–1012, 2010.

[16] Pierre-Amaury Grumiaux, Srđan Kitić, Laurent Girin, and Alexandre Guérin. A survey of sound source localization with deep learning methods. *The Journal of the Acoustical Society of America*, 152(1):107–151, 2022.

[17] Yufei Guo, Yuanpei Chen, Xiaode Liu, Weihang Peng, Yuhan Zhang, Xuhui Huang, and Zhe Ma. Ternary spike: Learning ternary spikes for spiking neural networks. *arXiv preprint arXiv:2312.06372*, 2023.

[18] Mark Horowitz. 1.1 computing's energy problem (and what we can do about it). In *2014 IEEE international solid-state circuits conference digest of technical papers (ISSCC)*, pages 10–14. IEEE, 2014. doi: 10.1109/isscc.2014.6757323 .

[19] Jie Hu, Li Shen, and Gang Sun. Squeeze-and-excitation networks. In *Proceedings of the IEEE conference on computer vision and pattern recognition*, pages 7132–7141, 2018.

[20] Eugene M Izhikevich. Simple model of spiking neurons. *IEEE Transactions on neural networks*, 14(6):1569–1572, 2003.

[21] Pingping Jiang, Christopher Kent, and Jonathan Rossiter. Towards sensory substitution and augmentation: Mapping visual distance to audio and tactile frequency. *Plos one*, 19(3):e0299213, 2024.

[22] Naim Kapucu and Vener Garayev. Collaborative decision-making in emergency and disaster management. *International Journal of Public Administration*, 34(6):366–375, 2011.

[23] Monika Körtje, Timo Stöver, Uwe Baumann, and Tobias Weissgerber. Impact of processing-latency induced interaural delay and level discrepancy on sensitivity to interaural level differences in cochlear implant users. *European Archives of Oto-Rhino-Laryngology*, 280(12):5241–5249, 2023.

[24] Souvik Kundu, Massoud Pedram, and Peter A Beerel. Hire-snn: Harnessing the inherent robustness of energy-efficient deep spiking neural networks by training with crafted input noise. In *Proceedings of the IEEE/CVF International Conference on Computer Vision*, pages 5209–5218, 2021.

[25] Bernhard Laback. Contextual lateralization based on interaural level differences is preshaped by the auditory periphery and predominantly immune against sequential segregation. *Trends in Hearing*, 27:23312165231171988, 2023.

[26] Peter Lakatos, Ankoor S Shah, Kevin H Knuth, Istvan Ulbert, George Karmos, and Charles E Schroeder. An oscillatory hierarchy controlling neuronal excitability and stimulus processing in the auditory cortex. *Journal of neurophysiology*, 94(3):1904–1911, 2005.

[27] Muhammad Usman Liaquat, Hafiz Suliman Munawar, Amna Rahman, Zakria Qadir, Abbas Z Kouzani, and MA Parvez Mahmud. Sound localization for ad-hoc microphone arrays. *Energies*, 14(12):3446, 2021.

[28] Jim-Shih Liaw and T.W. Berger. Robust speech recognition with dynamic synapses. In *1998 IEEE International Joint Conference on Neural Networks Proceedings. IEEE World Congress on Computational Intelligence (Cat. No.98CH36227)*, volume 3, pages 2175–2179 vol.3, 1998.

[29] Hong Liu, Yongheng Sun, Ge Yang, and Yang Chen. Binaural sound source localization based on weighted template matching. *CAAI Transactions on Intelligence Technology*, 6(2):214–223, 2021.

[30] Jindong Liu, David Perez-Gonzalez, Adrian Rees, Harry Erwin, and Stefan Wermter. A biologically inspired spiking neural network model of the auditory midbrain for sound source localisation. *Neurocomputing*, 74(1-3):129–139, 2010.

[31] Fran López-Caballero and Carles Escera. Binaural beat: a failure to enhance eeg power and emotional arousal. *Frontiers in human neuroscience*, 11:557, 2017.

[32] Alexandra Annemarie Ludwig, Sylvia Meuret, Rolf-Dieter Battmer, Marc Schönwiesner, Michael Fuchs, and Arne Ernst. Sound localization in single-sided deaf participants provided with a cochlear implant. *Frontiers in psychology*, 12:753339, 2021.

[33] Wolfgang Maass. Networks of spiking neurons: the third generation of neural network models. *Neural networks*, 10(9):1659–1671, 1997.

[34] Timothée Masquelier, Rudy Guyonneau, and Simon J Thorpe. Spike timing dependent plasticity finds the start of repeating patterns in continuous spike trains. *PloS one*, 3(1):e1377, 2008.

[35] Pavlo Molchanov, Stephen Tyree, Tero Karras, Timo Aila, and Jan Kautz. Pruning convolutional neural networks for resource efficient inference. *arXiv preprint arXiv:1611.06440*, 2016.

[36] Dylan Moore, Rebecca Currano, and David Sirkin. Sound decisions: How synthetic motor sounds improve autonomous vehicle-pedestrian interactions. In *12th International Conference on Automotive User Interfaces and Interactive Vehicular Applications*, pages 94–103, 2020.

[37] Fangli Ning, Jiahao Song, Jinglong Hu, and Juan Wei. Sound source localization of non-synchronous measurements beamforming with block hermitian matrix completion. *Mechanical Systems and Signal Processing*, 147:107118, 2021.

[38] Garrick Orchard, E Paxon Frady, Daniel Ben Dayan Rubin, Sophia Sanborn, Sumit Bam Shrestha, Friedrich T Sommer, and Mike Davies. Efficient neuromorphic signal processing with loihi 2. In *2021 IEEE Workshop on Signal Processing Systems (SiPS)*, pages 254–259. IEEE, 2021.

[39] Takashi Oya, Shohei Iwase, Ryota Natsume, Takahiro Itazuri, Shugo Yamaguchi, and Shigeo Morishima. Do we need sound for sound source localization? In *Proceedings of the Asian Conference on Computer Vision*, 2020.

[40] Zihan Pan, Malu Zhang, Jibin Wu, Jiadong Wang, and Haizhou Li. Multi-tone phase coding of interaural time difference for sound source localization with spiking neural networks. *IEEE/ACM Transactions on Audio, Speech, and Language Processing*, 29:2656–2670, 2021.

[41] Xinyuan Qian, Alessio Brutti, Oswald Lanz, Maurizio Omologo, and Andrea Cavallaro. Audio-visual tracking of concurrent speakers. *IEEE Transactions on Multimedia*, 24:942–954, 2021.

[42] Xinyuan Qian, Bidisha Sharma, Amine El Abridi, and Haizhou Li. Sloclas: A database for joint sound localization and classification. In *2021 24th Conference of the Oriental COCOSDA International Committee for the Co-ordination and Standardisation of Speech Databases and Assessment Techniques (O-COCOSDA)*, pages 128–133, 2021.

[43] Michael Risoud, J-N Hanson, Fanny Gauvrit, C Renard, P-E Lemesre, N-X Bonne, and Christophe Vincent. Sound source localization. *European annals of otorhinolaryngology, head and neck diseases*, 135(4):259–264, 2018.

[44] Zahra Roozbehi, Ajit Narayanan, Mahsa Mohaghegh, and Samaneh-Alsadat Saeedinia. Dynamic-structured reservoir spiking neural network in sound localization. *IEEE Access*, 2024.

[45] Bodo Rueckauer, Iulia-Alexandra Lungu, Yuhuang Hu, Michael Pfeiffer, and Shih-Chii Liu. Conversion of continuous-valued deep networks to efficient event-driven networks for image classification. *Frontiers in neuroscience*, 11:682, 2017. doi: 10.3389/fnins.2017.00682 .

[46] Daniel Schmid, Timo Oess, and Heiko Neumann. Listen to the brain–auditory sound source localization in neuromorphic computing architectures. *Sensors*, 23(9):4451, 2023.

[47] Thorben Schoepe, Daniel Gutierrez-Galan, Juan P Dominguez-Morales, Hugh Greatorex, Angel Jimenez-Fernandez, Alejandro Linares-Barranco, and Elisabetta Chicca. Closed-loop sound source localization in neuromorphic systems. *Neuromorphic Computing and Engineering*, 3(2):024009, 2023.

[48] Arda Senocak, Tae-Hyun Oh, Junsik Kim, Ming-Hsuan Yang, and In So Kweon. Learning to localize sound source in visual scenes. In *Proceedings of the IEEE Conference on Computer Vision and Pattern Recognition*, pages 4358–4366, 2018.

[49] Shihab A Shamma, Mounya Elhilali, and Christophe Micheyl. Temporal coherence and attention in auditory scene analysis. *Trends in neurosciences*, 34(3):114–123, 2011.

[50] Hwan Shim, Leah Gibbs, Karsyn Rush, Jusung Ham, Subong Kim, Sungyoung Kim, and Inyong Choi. Neural mechanisms related to the enhanced auditory selective attention following neurofeedback training: Focusing on cortical oscillations. *Applied sciences*, 13(14):8499, 2023.

[51] Joel S Snyder, Melissa K Gregg, David M Weintraub, and Claude Alain. Attention, awareness, and the perception of auditory scenes. *Frontiers in psychology*, 3:15, 2012.

[52] Paul Tarwireyi, Alfredo Terzoli, and Matthew O Adigun. Using multi-audio feature fusion for android malware detection. *Computers & Security*, 131:103282, 2023.

[53] Amirhossein Tavanaei, Masoud Ghodrati, Saeed Reza Kheradpisheh, Timothée Masquelier, and Anthony Maida. Deep learning in spiking neural networks. *Neural networks*, 111:47–63, 2019.

[54] Franziska Trede and Joy Higgs. Collaborative decision making. *Clinical reasoning in the health professions*, pages 43–54, 2008.

[55] Bernhard Vogginger, Felix Kreutz, Javier López-Randulfe, Chen Liu, Robin Dietrich, Hector A Gonzalez, Daniel Scholz, Nico Reeb, Daniel Auge, Julian Hille, et al. Automotive radar processing with spiking neural networks: Concepts and challenges. *Frontiers in neuroscience*, 16:851774, 2022.

[56] Kyriakos Voutsas and Jürgen Adamy. A biologically inspired spiking neural network for sound source lateralization. *IEEE transactions on Neural Networks*, 18(6):1785–1799, 2007.

[57] Julie A Wall, Liam J McDaid, Liam P Maguire, and Thomas M McGinnity. Spiking neural network model of sound localization using the interaural intensity difference. *IEEE transactions on neural networks and learning systems*, 23(4):574–586, 2012.

[58] Shuai Wang, Dehao Zhang, Ammar Belatreche, Yichen Xiao, Hongyu Qing, Wenjie We, Malu Zhang, and Yang Yang. Ternary spike-based neuromorphic signal processing system. *arXiv preprint arXiv:2407.05310*, 2024.

[59] Yabo Wang, Bing Yang, and Xiaofei Li. Fn-ssl: Full-band and narrow-band fusion for sound source localization. *arXiv preprint arXiv:2305.19610*, 2023.

[60] Wenjie Wei, Malu Zhang, Hong Qu, Ammar Belatreche, Jian Zhang, and Hong Chen. Temporal-coded spiking neural networks with dynamic firing threshold: Learning with event-driven backpropagation. In *Proceedings of the IEEE/CVF International Conference on Computer Vision*, pages 10552–10562, 2023.

[61] Wenjie Wei, Malu Zhang, Jilin Zhang, Ammar Belatreche, Jibin Wu, Zijing Xu, Xuerui Qiu, Hong Chen, Yang Yang, and Haizhou Li. Event-driven learning for spiking neural networks. *arXiv preprint arXiv:2403.00270*, 2024.

[62] John H Wittig Jr, Anthony I Jang, John B Cocjin, Sara K Inati, and Kareem A Zaghloul. Attention improves memory by suppressing spiking-neuron activity in the human anterior temporal lobe. *Nature Neuroscience*, 21(6):808–810, 2018.

[63] Zhimin Xu, Huicui Xin, Yuren Weng, and Guang Li. Hydrogeological study in tongchuan city using the audio-frequency magnetotelluric method. *Magnetochemistry*, 9(1):32, 2023.

[64] Bing Yang, Hong Liu, and Xiaofei Li. Srp-dnn: Learning direct-path phase difference for multiple moving sound source localization. In *ICASSP 2022-2022 IEEE International Conference on Acoustics, Speech and Signal Processing (ICASSP)*, pages 721–725. IEEE, 2022.

[65] Man Yao, Huanhuan Gao, Guangshe Zhao, Dingheng Wang, Yihan Lin, Zhaoxu Yang, and Guoqi Li. Temporal-wise attention spiking neural networks for event streams classification. In *Proceedings of the IEEE/CVF International Conference on Computer Vision*, pages 10221–10230, 2021. doi: 10.1109/iccv48922.2021.01006 .

[66] Man Yao, Guangshe Zhao, Hengyu Zhang, Yifan Hu, Lei Deng, Yonghong Tian, Bo Xu, and Guoqi Li. Attention spiking neural networks. *IEEE transactions on pattern analysis and machine intelligence*, 2023.

[67] Masahiro Yasuda, Yuma Koizumi, Shoichiro Saito, Hisashi Uematsu, and Keisuke Imoto. Sound event localization based on sound intensity vector refined by dnn-based denoising and source separation. In *ICASSP 2020-2020 IEEE International Conference on Acoustics, Speech and Signal Processing (ICASSP)*, pages 651–655. IEEE, 2020.

[68] Bojian Yin, Federico Corradi, and Sander M Bohté. Accurate and efficient time-domain classification with adaptive spiking recurrent neural networks. *Nature Machine Intelligence*, 3(10):905–913, 2021.

[69] Malu Zhang, Jiadong Wang, Jibin Wu, Ammar Belatreche, Burin Amornpaisannon, Zhixuan Zhang, Venkata Pavan Kumar Miriyala, Hong Qu, Yansong Chua, Trevor E Carlson, et al. Rectified linear postsynaptic potential function for backpropagation in deep spiking neural networks. *IEEE transactions on neural networks and learning systems*, 33(5):1947–1958, 2021.

[70] Xiaoli Zhong, Zihui Yang, Shengfeng Yu, Hao Song, and Zhenghui Gu. Comparison of sound location variations in free and reverberant fields: An event-related potential study. *The Journal of the Acoustical Society of America*, 148(1):EL14–EL19, 2020.

[71] Rui-Jie Zhu, Malu Zhang, Qihang Zhao, Haoyu Deng, Yule Duan, and Liang-Jian Deng. Tcja-snn: Temporal-channel joint attention for spiking neural networks. *IEEE Transactions on Neural Networks and Learning Systems*, 2024.

A RF Neurons for Energy Efficient FT alternative

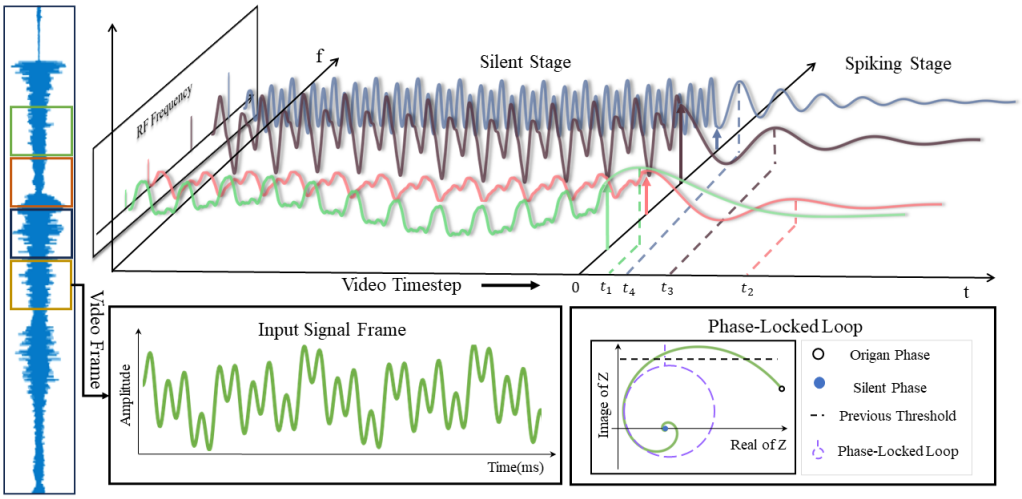

Figure 7: RF neurons serve as an energy-efficient alternative to FT, accumulating membrane potential during silent phases to substitute for FT, and directly mapping phases during spike phases.

Lemma 1. Nyquist Theorem
The Nyquist Theorem is pivotal for the sampling process in converting analog signals to digital signals. It stipulates that to avoid aliasing, the sampling frequency must be at least twice the maximum frequency component present in the analog signal. This criterion ensures that the reconstructed digital signal closely approximates the original analog signal without distortion.

Lemma 2. Fourier Transform (FT)
Consider an audio sequence $x = [x_1, x_2, \ldots, x_T]$ sampled at frequency f_s. The Fourier Transform (FT) facilitates the conversion from time domain to frequency domain, computed as:

$$\mathcal{F}[k] = \sum_{n=0}^{N-1} x[n] e^{-\mathrm{i}\frac{2\pi}{N}nk} = \sum_{n=0}^{N-1} x[n] \left(\cos\left(\frac{2\pi}{N}nk\right) - \mathrm{i}\sin\left(\frac{2\pi}{N}nk\right)\right), \tag{11}$$

where N is the number of discrete samples used in the FT. The complex vector $\mathcal{F}[k]$ quantifies the spectral components at varying frequencies. Utilizing Lemma 1, these components represent sinusoidal signals decomposed at frequencies indexed by k, scaled by $\frac{f_s}{N}$. For each component $\mathcal{F}[k] = a_k + ib_k$, the corresponding time-domain signal can be described by:

$$y_k(t) = \sqrt{a_k^2 + b_k^2} \sin\left(2\pi \frac{f_s}{N} kt + \tan^{-1}\left(\frac{b_k}{a_k}\right)\right). \tag{12}$$

Proof: Assume a series of RF neurons, each with a resonant frequency of $\omega = [-0 * \frac{2\pi}{N}, -1 * \frac{2\pi}{N}, -2 * \frac{2\pi}{N}, \ldots, -(N-1) * \frac{2\pi}{N}]$, initially set to zero. When exposed to a real-time input audio x, the response of the k^{th} neuron at time t is given by the recursive update:

$$\begin{aligned} Z_{\mathrm{RF}_k}[t] &= x[t] + \lambda e^{\mathrm{i}\omega_k \Delta t} Z_{\mathrm{RF}_k}[t-1] \\ &= x[t] + \lambda e^{\mathrm{i}\omega_k \Delta t}(x[t-1] + \lambda e^{\mathrm{i}\omega_k \Delta t} Z_{\mathrm{RF}_k}[t-2]) \\ &= \sum_{n=1}^{T} \lambda^n e^{\mathrm{i}n\omega_k \Delta t} x[t-n] = \sum_{n=1}^{T} \lambda^n \left(\cos\left(n\omega_k \Delta t\right) - \mathrm{i}\sin\left(n\omega_k \Delta t\right)\right) x[t-n]. \end{aligned} \tag{13}$$

This recursive filtering mimics a discrete Fourier transform when $\lambda = 1$. Moreover, RF neurons can be efficiently implemented on neuromorphic hardware like the Loihi2 chip, facilitating low-power and high-speed computations.

B Initial Oscillation Peak of RF Neurons as ITD Cue

Lemma 1. Neural Phase Coder
Inspired by observations of specific mechanisms within the auditory and visual cortices [9, 26], biological evidence are expressed through phase coding found. It can encode the pure tone audio into precise-timing spike. Regarding the results of the decomposition:

$$y_L = A_1 \sin\left(2\pi f_1 t + \tan^{-1}\left(\frac{b_{k_L}}{a_{k_L}}\right)\right), y_R = A_2 \sin\left(2\pi f_1 t + \tan^{-1}\left(\frac{b_{k_R}}{a_{k_R}}\right)\right), \tag{14}$$

y_L and y_R represent the single-tone sinusoidal signals arriving at the left and right ears. Subsequently, the first peak time is encoded into spike time as the arrival time of the sound.

$$t_L = \frac{1}{2\pi f}\left(\frac{\pi}{2} - \tan^{-1}\left(\frac{b_{k_L}}{a_{k_L}}\right)\right), t_R = \frac{1}{2\pi f}\left(\frac{\pi}{2} - \tan^{-1}\left(\frac{b_{k_R}}{a_{k_R}}\right)\right), \tag{15}$$

where f represents the frequency of the sinusoidal signal. Thus, ITD can be expressed as $t_L - t_R$.
Proof: When RF neurons (from both ears) enter the spike stage, their initial states are represented as $a_{k_L} + \mathrm{i}b_{k_L}$ for the left ear and $a_{k_R} + \mathrm{i}b_{k_R}$ for the right ear. Here, L indicates the left ear, R denotes the right ear, and K refers to the RF neuron associated with the intrinsic frequency f_k. Subsequently, the state will decay oscillations over time. To facilitate understanding, we calculate the real and imaginary parts in a discrete manner:

$$\begin{cases} a_{k_L}[t] = a_{k_L}[t-1]\cos(2\pi f_k) + b_{k_L}[t-1]\sin(2\pi f_k), \\ \\ b_{k_L}[t] = -a_{k_L}[t-1]\sin(2\pi f_k) + b_{k_L}[t-1]\cos(2\pi f_k)), \end{cases} \tag{16}$$

With the RF-PLC method we propose, we can directly spike timing acquisition. Specifically, RF neurons will fire spike at $a_{k_L}[t_{n_L}] = 0, b_{k_L}[t_{n_L}] = \max(b_{k_L})$. In the phase space, this state represented the first peak of time aligns with the neural phase coder:

$$\begin{cases} \phi_{locked} = \tan^{-1}\left(\dfrac{b_{k_L}[t_{n_L}]}{a_{k_L}[t_{n_L}]}\right) = \dfrac{\pi}{2}, & \text{Phase-locking Loop} \\ \\ \mathrm{ITD}_{RF} = t_{n_L} - t_{n_R} \approx t_L - t_R, & \text{RF-based ITD encoding} \end{cases} \tag{17}$$

where t_{n_L} satisfies $\phi_{locked} = \mathcal{Z}_{RF}[t_{n_L}]$ and t_{n_R} satisfies $\phi_{locked} = \mathcal{Z}_{RF}[t_{n_R}]$. Due to the discrete form, our ITD encodings are not identical to those in Lemma 1. The error is in the difference between the audio's sampling rate and the actual frequency. It results in our inability to accurately obtain the first peak time.

Specifically, as Lemma 1 demonstrates, to obtain the spike timing for pure tone audio of different frequencies, the phase coding model requires leveraging Eq.15 to compute the audio's ITD cues. However, with the RF-PLC method we propose, it can only iterate according to the audio's sampling rate. The difference between them is dependent on the sampling rate f_s, which can be represented as $1/f_s$. For the dataset SLoClas that we tested, its errors is only approximately 1%.

C Experiment Detail

We primarily validated the accuracy and robustness of our proposed method on the SLoClas dataset. It utilizes a 4-channel microphone array to collect data on RWCP sound scenes to ensure SNR of 40 to 50dB. It is comprised of ten distinct categories of ambient sounds: bells, bottles, buzzers, cymbals, horns, metal, particles, phones, rings, and whistles. Each category includes approximately 100 instances, providing a diverse and comprehensive set of audio samples.

Additional, to evaluate the robustness of our method, we need to construct source localization information under various complex scenarios. Specifically, we can introduce different types of noise into the audio. The noise sounds are sourced from the NOISEX-92 database, which contains recordings of various types of real-world noise. We add noise audio to each microphone channel to simulate noise coming from different directions.

$$ComplexVideo_i(n) = mic_i(n) + \lambda noise(n), i = 1, 2, 3, 4. \quad (18)$$

In this setup, $\text{mic}_i(n)$, where $i = 1, 2, 3, 4$, represents the 4-channel signals recorded by the microphone array. ComplexVideo_i denotes the multi-channel data with noise. The noise data consists of randomly selected audio clips from a noise database. λ is the scaling factor used to adjust the audio to a specific SNR ratio. A smaller SNR indicates a stronger noise presence in the audio which is more similar to real environment.

Table 3: Experimental configuration of the sound localization task.

Attributes	**Setup**
1. Data preprocessing:	
Sampling rate (Hz)	16000
Frame length (ms)	170
Frame stride (ms)	170
RF neurons n	512
Number of Microphones	4
2. RF-PLC setting:	
CQT frequency range (Hz)	[0, 8800]
τ (ms)	0.0625
Frequency channels N	40
Coincidence detector N_τ	51
Microphone pairs C	6
3. SNN Hyperparameter:	
α	0.75
Timestep	4
Epochs	300
Batch size	128
Optimizer	Adam
Base learning rate	1e-3
Learning rate decay	Cosine
Weight decay	5e-3

D Model Structure

The overall network architecture of our SNN-based SSL model is illustrated in Fig.8, featuring a comprehensive system design tailored for sound localization. The architecture consists of two main components: a front-end RF-PLC method and a back-end MAA-based localization decision network.

In the RF-PLC method, we utilize 512 RF neurons with widths ω that increase incrementally from 0 to 8000Hz. These neurons are strategically deployed as an alternative to the traditional FT operation, optimizing the model for energy efficiency and computational speed. Additionally, we utilize a cochlear filter bank following the Constant Q Transform (CQT) which is the most commonly used and easily implemented cochlear filter bank, to extract auditory features of appropriate dimensions. This encoding approach not only mimics the cochlear filtering process but also enhances the temporal dynamics of sound processing. Additionally, N detection neurons are engaged to characterize the ITD with delays ranging from -25τ to 25τ. Based on the audio sample ratio, the value of τ is set at 0.0625 ms. Furthermore, our model utilizes data from four microphones to compute ITDs between each pair, resulting in six distinct sets of ITD cues. As a result, each 170 ms speech frame is encoded into $X \in \mathbb{Z}^{C \times N \times N_\tau}$, capturing a rich array of spatial and temporal information. Details of these parameters can be found in Table.3. This setup ensures a detailed and dynamic spatial representation of auditory scenes.

In the back-end decision network, we propose a fully spike-based model, which is illustrated in Fig. 8. We will validate our module within the SSL models [7, 40] consisting of convolutional and MLP layers. To enhance the performance of the SSL model, we augment this basic structure with our MAA

module. This module is designed to emulate biological auditory processing by focusing on frequency band preference and short-term memory capabilities. Compared with traditional spatio-temporal spike attention techniques [65, 71], our module markedly improves the system's computational efficiency, as shown in Table. 2. Additionally, to better illustrate the performance of our module, we present a comparison with various modules. Details of these networks are provided in Table. 4. This enhancement allows for faster and more accurate sound localization, demonstrating the potential of our model in real-world applications.

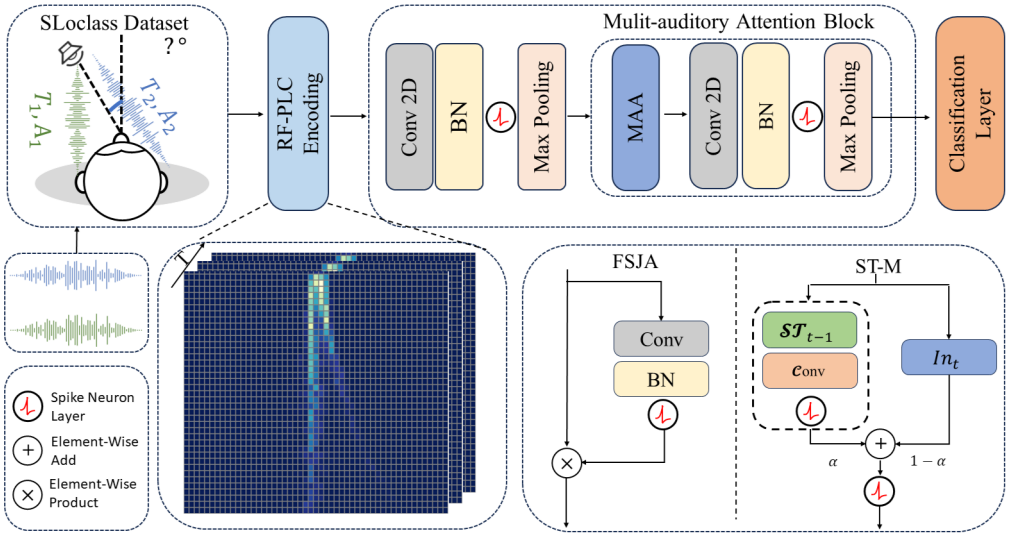

Figure 8: The structure of the Spike-based Neuromorphic Sound Source Localization. It includes an RF-PLC encoding method and a back-end classification model based on SNNs.

Table 4: Detail Network

Stage	Output Size	Baseline	Baseline + MAA	Baseline + others
Stage 1	$12 \times 25 \times 20$	Conv 3×3, stride 1 BatchNorm MaxPooling 2×2, stride 2		
Stage 2	$24 \times 12 \times 10$	Conv 3×3, stride 1 BatchNorm MaxPooling 2×2,stride 2	MAA module	other Attention
Stage 3	$48 \times 6 \times 5$	Conv 3×3, stride 1 BatchNorm MaxPooling 2×2,stride 2	MAA module	other Attention
Classifier	$1 \times 1 \times 1$		360-FC	

E Energy Cost

To describe the energy consumption calculations in the ablation experiments, we introduce a theoretical energy estimation method for the proposed attention mechanism. Compared to the ANN model, the energy consumption calculation of the spiking version requires information on the timesteps (T) and spike firing rates (R). The spike firing rate is defined as the proportion of non-zero elements in the spike tensor. Since our proposed MAA method is spike-driven, we only need to evaluate the model's FLOPs, along with T and R, to estimate the theoretical energy consumption of our methods.

In ANN [35], the FLOPs for the n-th Conv layer are expressed as:

$$\mathcal{C}onv = (k_n)^2 \cdot h_n \cdot w_n \cdot c_{n-1} \cdot c_n, \tag{19}$$

where k_n denotes the kernel size, (h_n, w_n) specifies the dimensions of the output feature map, and c_{n-1} and c_n represent the numbers of input and output channels, respectively. The FLOPs of the m-th MLP layer in ANNs are:

$$\mathcal{MLP} = i_m \cdot o_m, \tag{20}$$

where i_m and o_m represent the input and output dimensions of the m-th MLP layer.

Refer on previous research [24, 68], we assume that all computational data are implemented using 45nm technology for 32-bit floating-point calculations, with E_{MAC} = 4.6pJ and E_{AC} = 0.9 pJ.

In Table 3, we further present the details of different models. Referring to [66, 71], the attention matrix is derived using the sigmoid function, which results in the network input for the subsequent layer being non-spiking. Consequently, during the energy consumption calculation, this component is computed using the energy consumption of MAC operations, leading to a significant increase in energy consumption within the network. Due to the unique properties of the MAA attention matrix, our method does not introduce additional floating-point operations.

F Limitation

The limitations of this study include the lack of deployment on edge devices. Furthermore, the limited availability of datasets for SSL tasks restricts the validation of our model across a broader array of datasets. Future research will seek to overcome these challenges by amassing a more extensive collection of datasets and implementing our model on edge devices to more effectively ascertain the efficacy of our approach. The experimental results reported herein are reproducible, with detailed descriptions of the model architectures and hyperparameter configurations available in Appendix. Additionally, our code will be made available on subsequent after review.

G Supplementary Ablation Experiments

To further validate that the enhancement in our model's performance is indeed due to the effective implementation of band selection and short-term attention mechanisms, rather than an increased parameter count. We designed a Conv2d layer module with the same amount of parameters, ensuring all other parameters remained consistent. Specially,

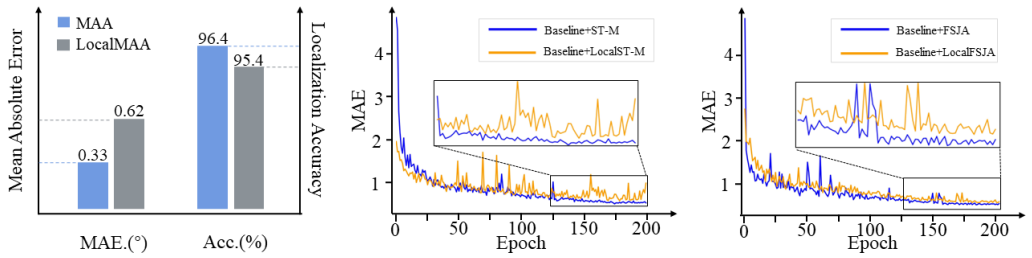

Figure 9: Supplemental ablation experiments. In these experiments, the Local module is configured with the same number of parameters as our proposed models to ensure a fair comparison: (a) A comparison of MAE.(°) and Acc.(%) between our proposed MAA and LocalMAA. (b) A comparison of the MAE between our proposed ST-M and LocalST-M. (c) A comparison of the MAE between FSJA and LocalFSJA.

As illustrated in Fig. 9, LocalMAA refers to a network with the same number of parameters as our proposed MAA. It can be observed that our MAA method achieves a lower MAE(°) and higher Acc(%). Furthermore, we compared the MAE of different modules, finding that our frequency band preference and short-term memory structure significantly enhance the network's localization performance.

NeurIPS Paper Checklist

1. **Claims**

   Question: Do the main claims made in the abstract and introduction accurately reflect the paper's contributions and scope?

   Answer: [Yes]

   Justification: Our abstract and introduction clearly describe our contribution, the algorithm, and the experimental results.

   Guidelines:

   - The answer NA means that the abstract and introduction do not include the claims made in the paper.
   - The abstract and/or introduction should clearly state the claims made, including the contributions made in the paper and important assumptions and limitations. A No or NA answer to this question will not be perceived well by the reviewers.
   - The claims made should match theoretical and experimental results, and reflect how much the results can be expected to generalize to other settings.
   - It is fine to include aspirational goals as motivation as long as it is clear that these goals are not attained by the paper.

2. **Limitations**

   Question: Does the paper discuss the limitations of the work performed by the authors?

   Answer: [Yes]

   Justification: We mentioned our limitation in Appendix. F

   Guidelines:

   - The answer NA means that the paper has no limitation while the answer No means that the paper has limitations, but those are not discussed in the paper.
   - The authors are encouraged to create a separate "Limitations" section in their paper.
   - The paper should point out any strong assumptions and how robust the results are to violations of these assumptions (e.g., independence assumptions, noiseless settings, model well-specification, asymptotic approximations only holding locally). The authors should reflect on how these assumptions might be violated in practice and what the implications would be.
   - The authors should reflect on the scope of the claims made, e.g., if the approach was only tested on a few datasets or with a few runs. In general, empirical results often depend on implicit assumptions, which should be articulated.
   - The authors should reflect on the factors that influence the performance of the approach. For example, a facial recognition algorithm may perform poorly when image resolution is low or images are taken in low lighting. Or a speech-to-text system might not be used reliably to provide closed captions for online lectures because it fails to handle technical jargon.
   - The authors should discuss the computational efficiency of the proposed algorithms and how they scale with dataset size.
   - If applicable, the authors should discuss possible limitations of their approach to address problems of privacy and fairness.
   - While the authors might fear that complete honesty about limitations might be used by reviewers as grounds for rejection, a worse outcome might be that reviewers discover limitations that aren't acknowledged in the paper. The authors should use their best judgment and recognize that individual actions in favor of transparency play an important role in developing norms that preserve the integrity of the community. Reviewers will be specifically instructed to not penalize honesty concerning limitations.

3. **Theory Assumptions and Proofs**

   Question: For each theoretical result, does the paper provide the full set of assumptions and a complete (and correct) proof?

   Answer: [Yes]

Justification: We mentioned our Theory Assumptions and Proofs in Section 3.1 and 3.2 and Appendix. A and B, respectively.

Guidelines:

- The answer NA means that the paper does not include theoretical results.
- All the theorems, formulas, and proofs in the paper should be numbered and cross-referenced.
- All assumptions should be clearly stated or referenced in the statement of any theorems.
- The proofs can either appear in the main paper or the supplemental material, but if they appear in the supplemental material, the authors are encouraged to provide a short proof sketch to provide intuition.
- Inversely, any informal proof provided in the core of the paper should be complemented by formal proofs provided in appendix or supplemental material.
- Theorems and Lemmas that the proof relies upon should be properly referenced.

4. **Experimental Result Reproducibility**

   Question: Does the paper fully disclose all the information needed to reproduce the main experimental results of the paper to the extent that it affects the main claims and/or conclusions of the paper (regardless of whether the code and data are provided or not)?

   Answer: [Yes]

   Justification: In the Appendix. C and D, we provide a detailed description of our model architecture and present all the training details, including dataset processing methods and hyperparameter settings.

   Guidelines:

   - The answer NA means that the paper does not include experiments.
   - If the paper includes experiments, a No answer to this question will not be perceived well by the reviewers: Making the paper reproducible is important, regardless of whether the code and data are provided or not.
   - If the contribution is a dataset and/or model, the authors should describe the steps taken to make their results reproducible or verifiable.
   - Depending on the contribution, reproducibility can be accomplished in various ways. For example, if the contribution is a novel architecture, describing the architecture fully might suffice, or if the contribution is a specific model and empirical evaluation, it may be necessary to either make it possible for others to replicate the model with the same dataset, or provide access to the model. In general. releasing code and data is often one good way to accomplish this, but reproducibility can also be provided via detailed instructions for how to replicate the results, access to a hosted model (e.g., in the case of a large language model), releasing of a model checkpoint, or other means that are appropriate to the research performed.
   - While NeurIPS does not require releasing code, the conference does require all submissions to provide some reasonable avenue for reproducibility, which may depend on the nature of the contribution. For example
     (a) If the contribution is primarily a new algorithm, the paper should make it clear how to reproduce that algorithm.
     (b) If the contribution is primarily a new model architecture, the paper should describe the architecture clearly and fully.
     (c) If the contribution is a new model (e.g., a large language model), then there should either be a way to access this model for reproducing the results or a way to reproduce the model (e.g., with an open-source dataset or instructions for how to construct the dataset).
     (d) We recognize that reproducibility may be tricky in some cases, in which case authors are welcome to describe the particular way they provide for reproducibility. In the case of closed-source models, it may be that access to the model is limited in some way (e.g., to registered users), but it should be possible for other researchers to have some path to reproducing or verifying the results.

5. **Open access to data and code**

Question: Does the paper provide open access to the data and code, with sufficient instructions to faithfully reproduce the main experimental results, as described in supplemental material?

Answer: [Yes]

Justification: We mentioned our data in the Appendix. D and code in supplemental material, respectively.

Guidelines:

- The answer NA means that paper does not include experiments requiring code.
- Please see the NeurIPS code and data submission guidelines (`https://nips.cc/public/guides/CodeSubmissionPolicy`) for more details.
- While we encourage the release of code and data, we understand that this might not be possible, so "No" is an acceptable answer. Papers cannot be rejected simply for not including code, unless this is central to the contribution (e.g., for a new open-source benchmark).
- The instructions should contain the exact command and environment needed to run to reproduce the results. See the NeurIPS code and data submission guidelines (`https://nips.cc/public/guides/CodeSubmissionPolicy`) for more details.
- The authors should provide instructions on data access and preparation, including how to access the raw data, preprocessed data, intermediate data, and generated data, etc.
- The authors should provide scripts to reproduce all experimental results for the new proposed method and baselines. If only a subset of experiments are reproducible, they should state which ones are omitted from the script and why.
- At submission time, to preserve anonymity, the authors should release anonymized versions (if applicable).
- Providing as much information as possible in supplemental material (appended to the paper) is recommended, but including URLs to data and code is permitted.

6. **Experimental Setting/Details**

   Question: Does the paper specify all the training and test details (e.g., data splits, hyperparameters, how they were chosen, type of optimizer, etc.) necessary to understand the results?

   Answer: [Yes]

   Justification: We provide the full details in Appendix. C and D.

   Guidelines:

   - The answer NA means that the paper does not include experiments.
   - The experimental setting should be presented in the core of the paper to a level of detail that is necessary to appreciate the results and make sense of them.
   - The full details can be provided either with the code, in appendix, or as supplemental material.

7. **Experiment Statistical Significance**

   Question: Does the paper report error bars suitably and correctly defined or other appropriate information about the statistical significance of the experiments?

   Answer: [Yes]

   Justification: We mentioned using random seeds to repeat at least 5 times to calculate the average in Table. 1 and 2.

   Guidelines:

   - The answer NA means that the paper does not include experiments.
   - The authors should answer "Yes" if the results are accompanied by error bars, confidence intervals, or statistical significance tests, at least for the experiments that support the main claims of the paper.
   - The factors of variability that the error bars are capturing should be clearly stated (for example, train/test split, initialization, random drawing of some parameter, or overall run with given experimental conditions).

- The method for calculating the error bars should be explained (closed form formula, call to a library function, bootstrap, etc.)
- The assumptions made should be given (e.g., Normally distributed errors).
- It should be clear whether the error bar is the standard deviation or the standard error of the mean.
- It is OK to report 1-sigma error bars, but one should state it. The authors should preferably report a 2-sigma error bar than state that they have a 96% CI, if the hypothesis of Normality of errors is not verified.
- For asymmetric distributions, the authors should be careful not to show in tables or figures symmetric error bars that would yield results that are out of range (e.g. negative error rates).
- If error bars are reported in tables or plots, The authors should explain in the text how they were calculated and reference the corresponding figures or tables in the text.

8. **Experiments Compute Resources**

   Question: For each experiment, does the paper provide sufficient information on the computer resources (type of compute workers, memory, time of execution) needed to reproduce the experiments?

   Answer: [Yes]

   Justification: We mentioned in the Appendix.C.

   Guidelines:

   - The answer NA means that the paper does not include experiments.
   - The paper should indicate the type of compute workers CPU or GPU, internal cluster, or cloud provider, including relevant memory and storage.
   - The paper should provide the amount of compute required for each of the individual experimental runs as well as estimate the total compute.
   - The paper should disclose whether the full research project required more compute than the experiments reported in the paper (e.g., preliminary or failed experiments that didn't make it into the paper).

9. **Code Of Ethics**

   Question: Does the research conducted in the paper conform, in every respect, with the NeurIPS Code of Ethics `https://neurips.cc/public/EthicsGuidelines`?

   Answer: [Yes]

   Justification: This paper strictly adheres to the NeurIPS Code of Ethics.

   Guidelines:

   - The answer NA means that the authors have not reviewed the NeurIPS Code of Ethics.
   - If the authors answer No, they should explain the special circumstances that require a deviation from the Code of Ethics.
   - The authors should make sure to preserve anonymity (e.g., if there is a special consideration due to laws or regulations in their jurisdiction).

10. **Broader Impacts**

    Question: Does the paper discuss both potential positive societal impacts and negative societal impacts of the work performed?

    Answer: [NA]

    Justification: This work is foundational research and not tied to particular applications.

    Guidelines:

    - The answer NA means that there is no societal impact of the work performed.
    - If the authors answer NA or No, they should explain why their work has no societal impact or why the paper does not address societal impact.
    - Examples of negative societal impacts include potential malicious or unintended uses (e.g., disinformation, generating fake profiles, surveillance), fairness considerations (e.g., deployment of technologies that could make decisions that unfairly impact specific groups), privacy considerations, and security considerations.

- The conference expects that many papers will be foundational research and not tied to particular applications, let alone deployments. However, if there is a direct path to any negative applications, the authors should point it out. For example, it is legitimate to point out that an improvement in the quality of generative models could be used to generate deepfakes for disinformation. On the other hand, it is not needed to point out that a generic algorithm for optimizing neural networks could enable people to train models that generate Deepfakes faster.
- The authors should consider possible harms that could arise when the technology is being used as intended and functioning correctly, harms that could arise when the technology is being used as intended but gives incorrect results, and harms following from (intentional or unintentional) misuse of the technology.
- If there are negative societal impacts, the authors could also discuss possible mitigation strategies (e.g., gated release of models, providing defenses in addition to attacks, mechanisms for monitoring misuse, mechanisms to monitor how a system learns from feedback over time, improving the efficiency and accessibility of ML).

11. **Safeguards**

    Question: Does the paper describe safeguards that have been put in place for responsible release of data or models that have a high risk for misuse (e.g., pretrained language models, image generators, or scraped datasets)?

    Answer: [NA]

    Justification: This paper poses no such risks.

    Guidelines:

    - The answer NA means that the paper poses no such risks.
    - Released models that have a high risk for misuse or dual-use should be released with necessary safeguards to allow for controlled use of the model, for example by requiring that users adhere to usage guidelines or restrictions to access the model or implementing safety filters.
    - Datasets that have been scraped from the Internet could pose safety risks. The authors should describe how they avoided releasing unsafe images.
    - We recognize that providing effective safeguards is challenging, and many papers do not require this, but we encourage authors to take this into account and make a best faith effort.

12. **Licenses for existing assets**

    Question: Are the creators or original owners of assets (e.g., code, data, models), used in the paper, properly credited and are the license and terms of use explicitly mentioned and properly respected?

    Answer: [Yes]

    Justification: Yes, the paper properly credits the creators or original owners of assets (e.g.,code, data, models) and explicitly mentions and respects the relevant licenses and terms of use.

    Guidelines:

    - The answer NA means that the paper does not use existing assets.
    - The authors should cite the original paper that produced the code package or dataset.
    - The authors should state which version of the asset is used and, if possible, include a URL.
    - The name of the license (e.g., CC-BY 4.0) should be included for each asset.
    - For scraped data from a particular source (e.g., website), the copyright and terms of service of that source should be provided.
    - If assets are released, the license, copyright information, and terms of use in the package should be provided. For popular datasets, `paperswithcode.com/datasets` has curated licenses for some datasets. Their licensing guide can help determine the license of a dataset.

- For existing datasets that are re-packaged, both the original license and the license of the derived asset (if it has changed) should be provided.
- If this information is not available online, the authors are encouraged to reach out to the asset's creators.

13. **New Assets**

    Question: Are new assets introduced in the paper well documented and is the documentation provided alongside the assets?

    Answer: [NA]

    Justification: No new assets are introduced in this article.

    Guidelines:

    - The answer NA means that the paper does not release new assets.
    - Researchers should communicate the details of the dataset/code/model as part of their submissions via structured templates. This includes details about training, license, limitations, etc.
    - The paper should discuss whether and how consent was obtained from people whose asset is used.
    - At submission time, remember to anonymize your assets (if applicable). You can either create an anonymized URL or include an anonymized zip file.

14. **Crowdsourcing and Research with Human Subjects**

    Question: For crowdsourcing experiments and research with human subjects, does the paper include the full text of instructions given to participants and screenshots, if applicable, as well as details about compensation (if any)?

    Answer: [NA]

    Justification: This paper does not involve crowdsourcing nor research with human subjects.

    Guidelines:

    - The answer NA means that the paper does not involve crowdsourcing nor research with human subjects.
    - Including this information in the supplemental material is fine, but if the main contribution of the paper involves human subjects, then as much detail as possible should be included in the main paper.
    - According to the NeurIPS Code of Ethics, workers involved in data collection, curation, or other labor should be paid at least the minimum wage in the country of the data collector.

15. **Institutional Review Board (IRB) Approvals or Equivalent for Research with Human Subjects**

    Question: Does the paper describe potential risks incurred by study participants, whether such risks were disclosed to the subjects, and whether Institutional Review Board (IRB) approvals (or an equivalent approval/review based on the requirements of your country or institution) were obtained?

    Answer: [NA]

    Justification: This paper does not involve crowdsourcing nor research with human subjects.

    Guidelines:

    - The answer NA means that the paper does not involve crowdsourcing nor research with human subjects.
    - Depending on the country in which research is conducted, IRB approval (or equivalent) may be required for any human subjects research. If you obtained IRB approval, you should clearly state this in the paper.
    - We recognize that the procedures for this may vary significantly between institutions and locations, and we expect authors to adhere to the NeurIPS Code of Ethics and the guidelines for their institution.
    - For initial submissions, do not include any information that would break anonymity (if applicable), such as the institution conducting the review.